

Josephson junction transmission lines as tunable artificial crystals

Carsten Hutter,¹ Kai Stannigel,^{1,2} Erik A. Tholén,³ Jack Lidmar,⁴ and David B. Haviland³

¹*Department of Physics, Stockholm University, AlbaNova University Center, SE-106 91 Stockholm, Sweden*

²*Institut für Theoretische Festkörperphysik, Universität Karlsruhe, D-76128 Karlsruhe, Germany*

³*Nanostructure Physics, Royal Institute of Technology, SE-106 91 Stockholm, Sweden*

⁴*Theoretical Physics, Royal Institute of Technology, SE-106 91 Stockholm, Sweden*

(Dated: January 30, 2022)

We investigate one-dimensional Josephson junction arrays with generalized unit cells, beyond a single junction or SQUID, as a circuit approach to engineer band gaps. Within a specific frequency range, of the order of the single junction plasma frequency, the dispersion relation becomes gapped and the impedance becomes purely imaginary. We derive the parameter dependence of this gap and suggest designs to lower it to microwave frequencies. The gap can be tuned in a wide frequency range by applying external flux, and persists in the presence of small imperfections. These arrays, which can be thought of as tunable artificial crystals, may find use in applications ranging from filters to the protection of quantum bits.

I. INTRODUCTION

The design of Josephson junction circuits in an appropriate electromagnetic environment¹ is currently of great interest in the context of superconducting qubits². Such qubits are *tunable artificial atoms*. In analogy, one can envision long, periodic arrays³ of Josephson junctions, which are engineered in order to achieve metamaterials, or *fully designable and tunable artificial crystals*. In this context, we study the physics of regular, one-dimensional Josephson junction arrays (1d-JJAs) with nontrivial unit cells, beyond a single junction or superconducting quantum interference device (SQUID).

Due to advances in fabrication techniques, regular JJAs have now gained renewed interest: 1d-JJAs have been the subject of study for the development of the 10 Volt Josephson voltage standard⁴, and were more recently investigated for a current standard^{5,6}, the transfer of quantum information⁷, and the readout and amplification of qubit signals^{8,9} at the quantum noise level¹⁰. 2d-JJAs have long been of interest in the context of quantum phase transitions¹¹, and were recently investigated in the context of negative permeability metamaterials^{12,13}.

Here we focus on the exploration of dispersion relations and band gaps, as known from condensed matter and crystal physics. Very recently, crystal physics with 1d-JJAs was studied in the regime where the Josephson junctions are treated as charge qubits¹⁴. We consider the opposite limit of junctions in the phase regime, which has the advantage that junctions have a comparatively large area and can therefore be fabricated with a low relative spread of parameters. Furthermore, we suggest two designs for which the band gap can be tuned by only one common applied magnetic field, which simplifies possible experiments. Junctions in the phase regime are approximately described by their linear behavior if the current flowing in the junctions is much less than the critical current. The array can then be regarded as a complex transmission line with a non-trivial, gaped dispersion relation. A resonator made with such a transmission line could find

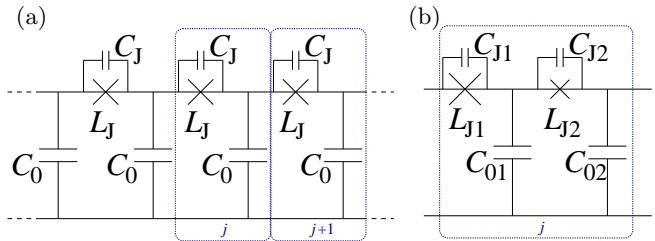


FIG. 1: (Color online) (a) A model of a regular 1d-JJA, where each unit cell j consists of a Josephson junction (modeled by tunnel element and capacitance) and a capacitance to ground. (b) A generalized model where each unit cell j consists of two different junctions and capacitances to ground.

use in circuit cavity QED^{15,16} for read-out of qubit signals. Nonlinear corrections to the model presented here can be used to realize parametric amplification^{8,9,10}.

We restrict ourselves to this linear regime, and focus on the possibilities of more complex unit cells and the parameter regimes achievable in realistic experiments. We begin our studies with a unit cell consisting of two junctions (or SQUIDs) with different parameters, as shown in Fig. 1b. In this case, we find a gap in the dispersion relation as shown in Fig. 2, i.e., a frequency region in which no propagating modes appear and the real part of impedance vanishes. This gap appears at frequencies of the order of the plasma frequencies of the individual junctions. We investigate the parameter dependence of the gap and possibilities to lower it to the experimentally accessible frequency region, appropriate for qubit design. We then discuss the connection between the real part of the impedance and the density of states for arbitrary unit cells in the linear regime. We present a general treatment which no longer requires the unit cells to be identical. We use this general approach to show that the gap persists in the presence of a small parameter spread (5% standard deviation), and present simulations for a transmission experiment with realistic boundary conditions.

II. JOSEPHSON JUNCTION ARRAYS WITH TWO-JUNCTION UNIT CELLS

A model of 1d-JJAs in the linear regime is shown in Fig. 1a, where each unit cell consists of a Josephson junction (with Josephson energy E_J and capacitance C_J), and a capacitance to ground C_0 . In the linear phase regime, one can further introduce the Josephson inductance as $L_J = \Phi_0^2/(4\pi^2 E_J)$, where Φ_0 is the superconducting flux quantum. L_J and C_J describe an intersite inductive and capacitive interaction, respectively, where we defined a site as the island between two junctions. The capacitance C_0 describes an onsite Coulomb interaction between Cooper pairs. We consider situations where resistive terms can be neglected. We note that in the limit $C_J \rightarrow 0$ the model reduces to the discrete, lumped element model of a transmission line for transverse electromagnetic waves. We start our studies with the generalization that the array consists of a lattice of unit cells each consisting of a basis of two Josephson junctions, for which we introduce an additional index 1 or 2 to the parameters above, see Fig. 1b.

Let us first discuss a special case included in the model: If we choose $C_{01} = C_{J2} = 0$ and regard L_{J2} as a geometric inductance instead of a Josephson inductance, we recover a model containing one junction and an additional inductance in series. This model was studied earlier, where the inductance L_0 was included in order to model the electromagnetic inductance of the JJA transmission line¹⁷. This inductance led to a gap in the real part of the impedance, taken between input port and ground¹⁷, which corresponds to a gap in the dispersion relation as shown in Fig. 2. However, for typical parameters the gap appeared at approximately 10^{11} - 10^{14} Hz. While the lower frequency could, in principle, be reduced by lowering the plasma frequency of the junction, the upper frequency extended beyond the range of validity of the simple Josephson junction model used. With our two-junction model, however, the upper band edge can be reduced in frequency by orders of magnitude.

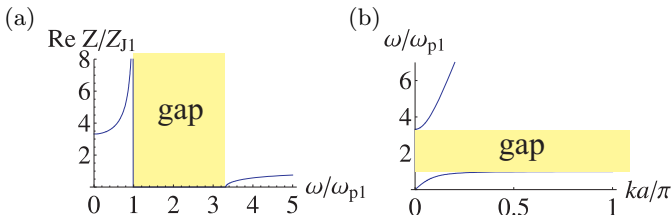


FIG. 2: (Color online) (a) Real part of the impedance and (b) dispersion relation. Both show a gap in the same frequency range. The impedance is normalized by $Z_{J1} = \sqrt{L_{J1}/C_{J1}}$ and the frequency is normalized by the plasma frequency $\omega_{p1} = 1/\sqrt{L_{J1}C_{J1}}$. The length of a unit cell is called a , and k is the wave number of a traveling wave solution. Here we used parameters $C_{J2} = C_{01} = 0$, where the model reduces to that of one junction and an additional inductance. Further, we chose parameters $C_{01}/C_{J1} = L_{J2}/L_{J1} = 0.1$.

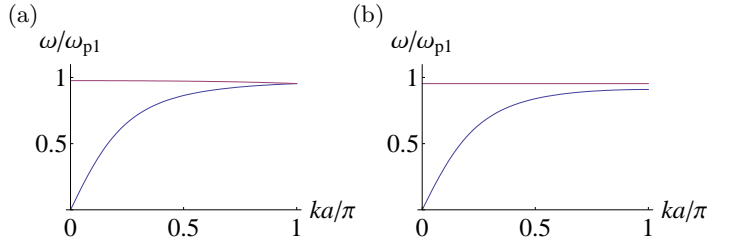


FIG. 3: (Color online) Dispersion relation for the model with two junctions when the junction parameters are (a) symmetric, $L_{J2}/L_{J1} = 1$, and (b) asymmetric, $L_{J2}/L_{J1} = 1.1$. In both cases we used $C_{J1} = C_{J2}$ and $C_{01}/C_{J1} = C_{02}/C_{J2} = 0.2$.

We shall now motivate the presence of this gap and then analyze its parameter dependence. First take an array with periodic boundary conditions and simple unit cells as in Fig. 1a, where each unit cell has only one degree of freedom due to loop constraints. Linearization of the equations of motion, in small value of phase difference across each junction, approximates the system as coupled harmonic oscillators. A traveling wave ansatz yields a single branch in the dispersion relation. This branch will have an upper cutoff frequency due to the discreteness of the model but no second branch and no gap. If we now consider new unit cells consisting of two original ones, each of the new cells has two independent degrees of freedoms. This results in a representation of the dispersion relation where the original branch is mirrored at half the Brillouin zone, and thus appears as two branches as shown in Fig. 3a. Here, we used the length a for the new unit cell. If an asymmetry of parameters is introduced within each unit cell, a splitting in the dispersion relation occurs as shown in Fig. 3b.

A geometric inductance $L_0 \ll L_J$ introduces a much stronger asymmetry, which explains the wide gap and experimentally inaccessible high frequency of the upper band edge (which tends to infinity for $L_0/L_J \rightarrow 0$) in the model of Ref. 17. With the two-junction model, we have a much wider parameter regime accessible, and can engineer the gap in a wide range.

As shown in the appendix, the dispersion relation is given as

$$[\omega_{\pm}(k)]^2 = \frac{B}{2A} \pm \frac{\sqrt{B^2 - 4AC}}{2A}, \quad (1)$$

where

$$\begin{aligned} A &= (C_{01} + C_{02})(C_{J1} + C_{J2}) + C_{01}C_{02} + C_{J1}C_{J2}\beta_k \\ B &= \frac{C_{01} + C_{02}}{L_{12}} + \left(\frac{C_{J1}}{L_{J2}} + \frac{C_{J2}}{L_{J1}}\right)\beta_k \\ C &= \frac{\beta_k}{L_{J1}L_{J2}}, \end{aligned} \quad (2)$$

with $1/L_{12} = 1/L_{J1} + 1/L_{J2}$ and $\beta_k = 2[1 - \cos(ka)]$. Since $A > 0$, one sees from the defining Eq. (1) that $\omega_+(k) \geq \omega_-(k)$ for any wave vector k . The lower and

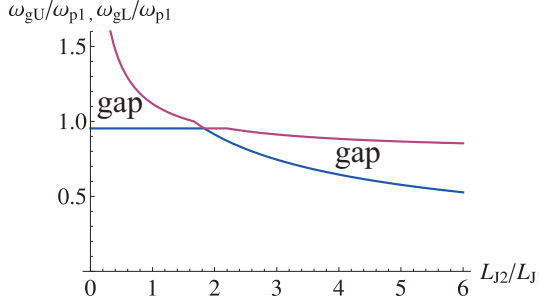


FIG. 4: (Color online) The upper and lower band edge in dependence of the ratio L_2/L_1 . We used $C_{J2}/C_{J1} = 0.5$ and $C_{01} = C_{02} = 0.2C_{J1}$.

upper edge of the gap are defined as

$$\begin{aligned}\omega_{gL} &= \max_k \{\omega_-(k)\}, \\ \omega_{gU} &= \min_k \{\omega_+(k)\},\end{aligned}\quad (3)$$

respectively. One finds that, for realistic parameters, the lower band edge always appears at wave vectors $ka = \pi$, where $\beta_k = 4$, while the upper band edge can appear at $ka = 0$ or $ka = \pi$, depending on the parameters, cf. Figs. 2b and 3b. In the first case, the upper band edge reduces to $\omega_+(0) = 1/\sqrt{L_{12}C_\Sigma}$, where we defined $C_\Sigma = C_{J1} + C_{J2} + C_{01}C_{02}/(C_{01} + C_{02})$. We show in Fig. 4 how the gap can be moved in frequency if one can control the ratio of effective Josephson inductances L_{J2}/L_{J1} . The gap vanishes, $\omega_{gL} = \omega_{gU}$, if both $C_{01} = C_{02} \equiv C_0$ and

$$L_{J1}C_{J1} = L_{J2}C_{J2} + C_0(L_{J2} - L_{J1}). \quad (4)$$

Kinks in the plot appear at the points, where the upper branch $\omega_+(k)$ switches minima between $k = 0$ and $k = a/\pi$. This happens for either of the two conditions

$$\begin{aligned}\frac{L_{J2}}{L_{J1}} &= \frac{C_{01}C_{J1} + C_{02}C_{J1} + C_{01}C_{02}}{(C_{01} + C_{02})C_{J2}}, \\ \frac{L_{J2}}{L_{J1}} &= \frac{(C_{01} + C_{02})C_{J1}}{C_{01}C_{02} + C_{01}C_{J2} + C_{02}C_{J2}}.\end{aligned}\quad (5)$$

Such tunable inductances can be achieved by replacing one or both junctions in each unit cell by a SQUID, which consists of two junctions with Josephson energy E_{J0} , and which is pierced by a magnetic field B . The Josephson energy, which is inversely proportional to the Josephson inductance, can then be controlled as $E_J = 2E_{J0} \cos(2\pi|B|A_S/\Phi_0)$. Here, A_S is the effective area of the SQUID with respect to the B -field. A design with one junction and one SQUID per unit cell has the advantage that one of the two inductances can be tuned continuously without changing the other inductance. A design with two SQUIDs per unit cell has different advantages. Clearly, one can then tune both Josephson energies. If one chooses different areas A_{S1} and A_{S2} for the two SQUIDs, a change in magnetic field $\Delta B = \Phi_0/A_{S1}$ leaves the Josephson energy of the first SQUID invariant,

while it changes that of the second SQUID. In this sense, one can tune both Josephson energies independently with only one common magnetic field. Thus, this design is preferable in experiments which test many combinations of inductances (L_{J1}, L_{J2}) , while the aforementioned design is better if one needs a continuous change of one inductance, which might become important for applications.

III. MORE GENERAL UNIT CELLS

Here, we will clarify why the real part of the impedance and the dispersion relation are connected as presented in Fig. 2, and show that this connection is of more general nature. At the same time, we will provide formulas which can also be used in the case of more general types of unit cells (e.g. with three or more different Josephson junctions or SQUIDs) and for the investigation of parameter spreads.

If we allow an arbitrary combination of capacitances, inductances and Josephson junctions, the Lagrangian in the linear regime can always be written as

$$L = \sum_{j,k=1}^M [\dot{\Phi}_j \frac{C_{jk}}{2} \dot{\Phi}_k - \Phi_j \frac{(L^{-1})_{jk}}{2} \Phi_k] \quad (6)$$

Here, M is the total number of independent variables, and Φ_j are independent flux variables. In the case of the two-junction unit cell we had $M = 2N$, with N the number of unit cells, and as variables we used the integrated voltage at the capacitances to ground, $\Phi_j = \int_{-\infty}^t V_j(t') dt'$. Further, \mathbf{C} is the capacitance matrix and \mathbf{L}^{-1} is the inverse inductance matrix, which can contain both the kinetic inductance due to Josephson junctions and the geometric inductance. This is a problem of coupled harmonic oscillators, which can be diagonalized by the transformation $\Phi \rightarrow \tilde{\Phi} = \mathbf{U}^T \mathbf{C}^{1/2} \Phi$. Here we took into account that the matrices \mathbf{C} and \mathbf{L} can always be chosen symmetric, and defined \mathbf{U} as the matrix which has rows consisting of the normalized, real eigenvectors of the matrix $\Omega^2 \equiv \mathbf{C}^{-1/2} \mathbf{L}^{-1} \mathbf{C}^{-1/2}$. The transformed Lagrangian is given as $\tilde{L} = \frac{1}{2} \sum_{j=1}^N [\dot{\tilde{\Phi}}_j^2 - \omega_j^2 \tilde{\Phi}_j^2]$, where we introduced the eigenvalues ω_j^2 of Ω^2 .

The equations of motion in this eigenbasis are decoupled and given as $\ddot{\tilde{\Phi}}_j = -\omega_j^2 \tilde{\Phi}_j$. For the model with a two-junction unit cell, the connection to the dispersion relation is shown in Fig. 5. Here we sorted the eigenfrequencies ω_j , grouped them in a lower and higher frequency set with same number of frequencies, and plotted them equally spaced. They resemble the dispersion relation for a regular array, and can still be calculated in the presence of imperfections as shown in section IV.

The Hamiltonian corresponding to the transformed Lagrangian is given as $H = \frac{1}{2} \sum_j (\tilde{Q}_j^2 + \omega_j^2 \tilde{\Phi}_j^2)$, where $\tilde{Q}_j = \dot{\tilde{\Phi}}_j$ is the conjugate variable to $\tilde{\Phi}$. For later convenience, this Hamiltonian can be rewritten in the standard

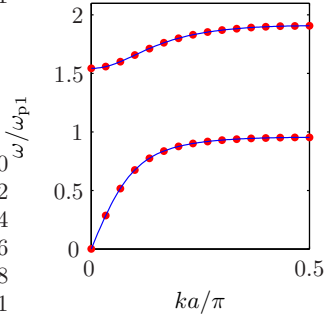


FIG. 5: (Color online) Dispersion relation (solid line) calculated by Eq. (1), and ordered eigenfrequencies ω_j (dots) calculated by diagonalization of the matrix Ω , for a finite array with two-junction unit cell. Here, we used parameters $L_{J2} = 0.25L_{J1}$ and $C_{01} = C_{02} = 0.2C_1 = 0.2C_2$ which lead to a wider gap than in Fig. 3b.

form $H = \sum_{j=1}^N \hbar\omega_j(a_j^\dagger a_j + \frac{1}{2})$ when creation and annihilation operators are defined by the equations

$$\begin{aligned}\tilde{\Phi}_j &= \sqrt{\hbar/(2\omega_j)}(a_j^\dagger + a_j) , \\ \tilde{Q}_j &= i\sqrt{\hbar\omega_j/2}(a_j^\dagger - a_j) .\end{aligned}\quad (7)$$

Now we proceed to consider the connection between the real part of the impedance, the density of states and the dispersion relation. For the frequency range at which the dispersion relation shows a gap, there are no undamped, propagating modes and hence no transmission (in the limit of an infinite array). Then all signals are reflected back and the impedance becomes purely imaginary. In general, the real part of impedance can be expressed via the fluctuation dissipation theorem¹⁸ as

$$\text{Re } Z(\omega) = \frac{1}{2\hbar\omega}(1 - e^{-\beta\hbar\omega})S_V(\omega) . \quad (8)$$

Here, the spectral density is given as $S_V(\omega) = \int_{-\infty}^{\infty} \langle V(t)V(0) \rangle e^{i\omega t} dt$, where the voltage operator is given in the Heisenberg representation, $V(t) = e^{iHt/\hbar}V e^{-iHt/\hbar}$, and we assume a Boltzmann distribution for the averaging, $\langle \mathcal{O} \rangle = \text{Tr}(e^{-\beta H}\mathcal{O})/\mathcal{Z}$ with $\mathcal{Z} = \text{Tr}(e^{-\beta H})$. Evaluating the trace in the energy eigenbasis $H|n\rangle = E_n|n\rangle$ yields

$$S_V(\omega) = \frac{1}{\mathcal{Z}} \sum_{m,n} e^{-\beta E_n} |\langle m|V|n\rangle|^2 \delta(\omega - \frac{E_m - E_n}{\hbar}) . \quad (9)$$

In the case of a Hamiltonian consisting of M decoupled harmonic oscillators discussed above, the states $|n\rangle$ and $|m\rangle$ are product states, and the energies E_n and E_m depend on the occupation numbers of these states. For example, the energy of the state $|n\rangle = \prod_{j=1}^M |n_j\rangle$ is

$$E_n = \sum_{j=1}^M \epsilon_j(n_j + \frac{1}{2}) . \quad (10)$$

We shall assume sufficient spread of capacitances and inductances in an experiment, such that we do not have to consider degeneracies of the energies $\epsilon_j \equiv \hbar\omega_j$. The operator of voltage in Eq. (9) is in general a superposition $V = \sum_k \beta_k \hat{\Phi}_k$, where the coefficients β_k are dependent on the specific system under consideration. The voltage operator can then be rewritten as $V = \sum_j \alpha_j \sqrt{2\hbar\omega_j}(a_j^\dagger - a_j)$, with coefficients $\alpha_j = \frac{i}{2} \sum_{k,l} \beta_k (C^{-1/2})_{k,l} U_{l,j}$.

It is then straight forward to calculate the matrix elements $|\langle m|V|n\rangle|^2$ in Eq. (9) to get

$$S_V(\omega > 0) = \left(\frac{2\hbar\omega}{1 - e^{-\beta\hbar\omega}} \right) \sum_j |\alpha_j|^2 \delta(\omega - \epsilon_j/\hbar) . \quad (11)$$

Using Eq. (8), the real part of the impedance is given as

$$\text{Re } Z(\omega > 0) = \sum_j |\alpha_j|^2 \delta(\omega - \epsilon_j/\hbar) . \quad (12)$$

The delta-function on the right side of the equation picks out only terms in the sum over j for which $\epsilon_j = \hbar\omega$. The real part of the impedance is thus given as number of states per frequency (related to the dispersion relation as discussed for Fig. 5), multiplied by a weight factor $|\alpha_j|^2$ which depends on the distribution of capacitances and inductances in the circuit.

IV. EXPERIMENTAL CONSIDERATIONS

A. Range of validity and experimental parameters

The two branches in the dispersion relation and the associated gap in frequency, where no propagating modes exist in the JJA transmission line, could be a very useful property for the design of quantum circuits in the microwave region. The essential ingredient for realizing this gap is an asymmetry in the parameters for each of two junctions in the basis of the periodic structure. Furthermore, in the parameter regime $C_{J1}, C_{J2} \gg C_{01}, C_{02}$, the gap is vanishing or small when the plasma frequencies of the two junctions are the same. One should thus aim for parameters $\omega_{p1} \neq \omega_{p2}$ in order to observe the gap. When fabricating JJAs, typically all junctions are made in the same process step, resulting in a tunnel barrier which is nearly uniform across the entire chip or wafer. In this case, the ratio $\sqrt{L_J/C_J}$ will be inversely proportional to the junction area, and the plasma frequency $\omega_p = 1/\sqrt{L_J C_J}$ will be independent of the junction area. Thus, simply changing the junction area in the fabrication process will not achieve the desired goal.

Subject to the constraint of uniform tunnel barriers, there are basically two ways to change the plasma frequency, and both bring it down in frequency. The first method is to increase L_J of one of the junctions by forming a SQUID loop of this junction and applying an external magnetic flux. This method is attractive because changing the external flux corresponds to tuning

the frequency range of the transmission gap. However, with this approach, dropping the plasma frequency corresponds to dropping the critical current of the transmission line, and therefore non-linear corrections will become important at much lower power. Furthermore, when increasing L_J such that the transmission line impedance $\sqrt{L_J/C_0}$ becomes large compared to the quantum resistance $R_Q = h/4e^2 = 6.45\text{k}\Omega$, one finds that large quantum fluctuations of the phase result in a Coulomb blockade, and our assumption of classical phase dynamics has completely broken down¹⁹.

The second possibility to drop the plasma frequency is to fabricate an on-chip capacitance in parallel with each junction which must be very close to each junction, so that a lumped element capacitance is a good approximation at high frequencies. This route will not cause a degradation of critical current, however, it does require more layers of lithography than the simple single layer process used in the shadow deposition technique. Fabrication with the Nb trilayer technique however provides this parallel capacitance naturally, and it can easily be designed by simple modification of the masks used for the lithography²⁰. By combining this technique and applied fluxes, we estimate that the plasma frequencies can be brought into the experimentally accessible parameter regime, of order 10 Ghz, which would allow for observation of the gap.

B. Influence of parameter spread and transmission

So far, we assumed that junctions can be fabricated identically if desired. However, in reality, there will be a spread of junction parameters in the fabrication. We expect that the gap in the spectrum, impedance and transmission will persist provided that the disorder is weak enough and/or the array is short enough that localization effects can be ignored. Here we consider in more detail the influence of parameter spread on the validity of our results. In that case, the condition of periodicity is lost, and wave vectors as in Fig. 5 are not well-defined. However, it is still possible to investigate the density of states, which is shown in Fig. 6a,b. Here we counted the number of states in a discretized frequency interval. The parameters in all parts of Fig. 6 are the same as in Fig. 5, except that we used a spread of Josephson inductances of $\pm 5\%$ in Fig. 6b,d,f and considered 500 unit cells in the case of Fig. 6a,b in order to count a reasonable number of states. Despite the spread in parameters a gap can still be clearly observed in the density of states.

In an experiment, it is easier to measure transmission than the dispersion itself. Furthermore, realistic boundary conditions become important for a real experiment. In Fig. 6c,d we show the transmission for a finite array with realistic boundary conditions, i.e., a connection to input and output leads, which themselves are connected to ground via input and output impedances Z_{in} and Z_{out} of 50Ω . While this setup is not a cavity,

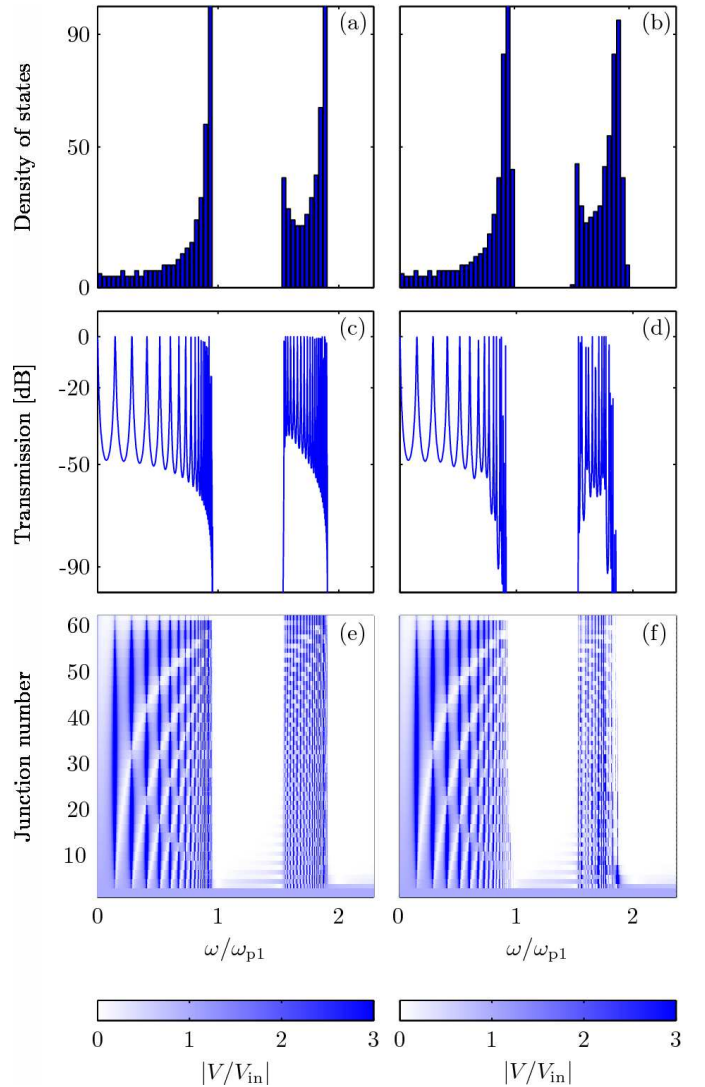


FIG. 6: (Color online) (a),(b) Density of states. (c),(d) Transmission. (e),(f) Voltage at the sites. In parts (b), (d), and (f), a $\pm 5\%$ spread in Josephson inductances is used. Further, $L_{J2} = 0.25L_{J1}$, $C_{01} = C_{02} = 0.2C_1 = 0.2C_2$, $Z_{\text{in}} = Z_{\text{out}}$, and $Z_{\text{in}}/\sqrt{L_{J1}/C_{J1}} = 50 \cdot 10^{-5/2}$.

it behaves like a resonator because the impedances are not matched. Indeed, the voltage differences between the sites and ground resemble standing waves (up to the discreteness), as can be seen in Fig. 6e,f, which is like Fig. 6c,d obtained with classical circuit theory. For frequencies inside the gap region, the transmission drops drastically which can be understood by an exponential decay of voltage amplitude at the sites (comparing same sites of different unit cells). While the gap becomes less sharp in the presence of a parameter spread, it can still be clearly seen in the transmission. An experiment of this sort appears therefore very promising.

V. SUMMARY AND OUTLOOK

We theoretically investigated regular Josephson junction arrays with generalized unit cells, e.g., unit cells consisting of two junctions with different parameters. In the linear approximation of the phase regime, we found a gap in the dispersion relation and in the real part of the impedance, when considered over frequency. This gap is not present in the linear regime of models with only one junction per unit cell, unless additional circuit elements in each unit cell are used. We derived the parameter dependence of the gap, and found that for a design with two different Josephson junctions, it appears at frequencies of the same order of magnitude as the plasma frequencies of the two junctions. We suggested how to lower these frequencies in an experimental setup in order to shift the gap to an accessible frequency range. By replacing one of the two junctions per unit cell with a SQUID, the gap can be tuned in situ. Furthermore, we derived the connection between the real part of the impedance and the dispersion relation for more general unit cells, and found expressions which can be used when the periodicity condition is lifted. Using these expressions we showed that the gap persists upon a realistic parameter spread of the junctions, both in the density of states and in a transmission experiment with realistic boundary conditions.

Our results could on the one hand be used for comparatively simple demonstration of tunable artificial crystals with Josephson junctions, which is interesting from the point of view of fundamental physics. On the other hand, such tunable artificial crystals, embedded in superconducting structures, could become important for new types of applications, for example, for specific types of frequency filters.

One could also envision to protect qubits against decoherence with such JJs, by placing a Cooper pair box qubit in the middle of two of them. If the energy splitting of the qubit lies inside the region of the gap, where no traveling modes are available, we expect the dissipation of the qubit to be strongly suppressed. One should note that the decoherence of a qubit is composed not only of the relaxation but also of the pure dephasing, and the time scale of the latter is typically the critical, shorter one. On the other hand, recent experiments reached extremely high decoherence times, which at least for part of the frequency range appeared to be limited by the relaxation²¹. In this case, suppressing of the relaxation would allow refined studies on remaining sources of decoherence.

The most immediate use of JJs with nontrivial unit cells could be a modification of the frequency range of superconducting parametric amplifiers, which recently have already been fabricated with unit cells consisting of SQUIDs⁹.

APPENDIX A: DERIVATION OF THE DISPERSION RELATION.

The Lagrangian for the model consisting of unit cells with two types of Josephson junctions (Fig. 1b) is given as

$$\begin{aligned} L_2 = & \sum_{j=0}^{N-1} \left[\frac{C_{0,1}}{2} \dot{\Phi}_{j,1}^2 + \frac{C_{0,2}}{2} \dot{\Phi}_{j,2}^2 \right] \\ & + \sum_{j=0}^{N-1} \left[\frac{C_{J1}}{2} (\dot{\Phi}_{j-1,2} - \dot{\Phi}_{j,1})^2 + \frac{C_{J2}}{2} (\dot{\Phi}_{j,1} - \dot{\Phi}_{j,2})^2 \right] \\ & + \sum_{j=0}^{N-1} [E_{J1} \cos(\phi_{j-1,2} - \phi_{j,1}) + E_{J2} \cos(\phi_{j,1} - \phi_{j,2})], \end{aligned} \quad (A1)$$

where we eliminated the Josephson phases $\phi_{J,j}$ and defined fluxes and phases $\Phi_{j,1/2} = \Phi_0 \phi_{j,1/2} / 2\pi$ at the capacitors to ground.

From this Lagrangian, one can find the equations of motion, and, after the linear approximation, $\phi_{J,j} \ll 1$, make a traveling wave ansatz,

$$\begin{pmatrix} \Phi_{J1} \\ \Phi_{J2} \end{pmatrix} = \begin{pmatrix} u \\ v e^{ika/2} \end{pmatrix} e^{i(k ja - \omega t)}. \quad (A2)$$

Here, we introduced a length a for the total unit cell, which results in a factor $a/2$ for a single junction. The equations of motion can be rewritten as a matrix \mathbf{M} multiplying the vector $(u, v)^T$ such that $\mathbf{M}(u, v)^T = 0$. Nontrivial solutions exist only when the determinant of \mathbf{M} is zero, which results in the dispersion relation stated in Eq. (1).

ACKNOWLEDGMENTS

We thank Hans Hansson for valuable discussions and comments on the manuscript. This work was supported by the Swedish Research Council (VR) and by NordForsk.

¹ G. Schön and A.D. Zaikin, Phys. Rep. **198**, 237 (1990)

² Yu. Makhlin, G. Schön, and A. Shnirman, Rev. Mod. Phys. **73**, 357 (2001).

³ R.M. Bradley and S. Doniach, Phys. Rev. B **30**, 1138 (1984).

⁴ R. L. Kautz, Rep. Prog. Phys. **59**, 935 (1996)

⁵ J. Bylander, T. Duty, and P. Delsing, Nature **434**, 361 (2005).

⁶ M. Cholascinski and R. W. Chhajlany, Phys. Rev. Lett. **98**, 057004 (2007).

⁷ A. Romito, R. Fazio, and C. Bruder, PRB **71**, 100501(R) (2005)

⁸ E. A. Tholén, A. Ergül, E. M. Doherty, F. M. Weber, F. Grégis, and D. B. Haviland, Appl. Phys. Lett. **90**, 253509 (2007).

⁹ M. A. Castellanos-Beltran and K. W. Lehnert, Appl. Phys. Lett. **91**, 083509 (2007).

¹⁰ B. Yurke, P. G. Kaminsky, R. E. Miller, E. A. Whittaker, A. D. Smith, A. H. Silver, and R. W. Simon, Phys. Rev. Lett. **60**, 764 (1988).

¹¹ R. Fazio, H. van der Zant, Phys. Rep. **355**, 235 (2001)

¹² C. Du, H. Chen, and S. Li, Phys. Rev. B **74**, 113105 (2006).

¹³ N. Lazarides and G. P. Tsironis, Appl. Phys. Lett. **90**, 163501 (2007).

¹⁴ A.L. Rakhmanov, A.M. Zagoskin, Sergey Savel'ev, and Franco Nori, arXiv:0709.1314

¹⁵ A. Wallraff, D. I. Schuster, A. Blais, L. Frunzio, R.-S. Huang, J. Majer, S. Kumar, S. M. Girvin, and R. J. Schoelkopf, Nature **431**, 162 (2004).

¹⁶ D. I. Schuster, A. A. Houck, J. A. Schreier, A. Wallraff, J. M. Gambetta, A. Blais, L. Frunzio, B. Johnson, M. H. Devoret, S. M. Girvin, and R. J. Schoelkopf, Nature **445**, 515 (2007).

¹⁷ D. B. Haviland, K. Andersson, and P. Ågren, J. Low Temp. Phys. **118**, 733 (2000).

¹⁸ H. Nyquist, PR **32**, 110 (1928).

¹⁹ E. Chow, P. Delsing and D.B. Haviland, PRL 81, 204 (1998)

²⁰ R. Dolata, H. Scherer, A.B. Zorin, and J. Niemeyer, J. Appl. Phys. **97**, 054501 (2005).

²¹ J. A. Schreier, A. A. Houck, J. Koch, D. I. Schuster, B. R. Johnson, J. M. Chow, J. M. Gambetta, J. Majer, L. Frunzio, M. H. Devoret, S. M. Girvin, R. J. Schoelkopf, arXiv:0712.3581